Measurement of 6-DOF Displacement of Rigid Bodies through Splitting a Laser Beam: Experimental Investigation

W. S. Park [a], H. S. Cho [b], Y. K. Byun [c], and N. Y. Park [c]

[a] Central R&D Center, Mando Corporation
343-1, Manho-ri, Poseung-myun, Pyungtaek 451-821, Korea

[b] Department of Mechanical Engineering, Korea Advanced Institute of Science and Technology
373-1, Kusong-dong, Yusong-gu, Taejeon 305-701, Korea

[c] Samsung Advanced Institute of Technology
P.O. Box 111, Suwon 440-600, Korea

ABSTRACT

In this paper, a new measuring system is proposed which can measure 6-DOF motion of rigid bodies. Its measurement principle is based on detection of laser beam reflected from a specially fabricated mirror whose shape is a triangular pyramid having an equilateral cross-sectional shape. The 3-facet mirror is mounted on the object whose 6-DOF displacement is to be measured. The measurement is operated by a laser-based optical system composed of a 3-facet mirror, a laser source, three position-sensitive detectors(PSD). In the sensor system, three PSDs are located at three corner points of a triangular formation, which is an equilateral triangular formation lying parallel to the reference plane. From this arrangement, 6-DOF displacement of any object can be simply determined. In this paper, we model the relationship between the 6-DOF displacement of the object and the outputs of three PSDs. A series of experiments is performed to demonstrate the effectiveness of the proposed method. The experimental results show that the proposed sensing system can be an effective means of obtaining 3-dimensional position and orientation of arbitrary objects.

Keywords: 3-dimensional pose, 6-DOF motion, 3-facet mirror, optical metrology, position-sensitive detector

1. INTRODUCTION

A rigid body, which is not constrained to any kinematic condition, has six degrees of kinematic freedom in space. Therefore, it needs six spatial parameters such as x, y, z in translation and roll, pitch, yaw in rotation to fully describe the 3-dimensional position and orientation of a rigid body. In order to simultaneously measure the 3-dimensional position and orientation of rigid bodies, a lot of approaches have been proposed such as computer vision, 6-DOF master devices in master-slave mechanisms, inertial navigation system(INS).

Computer vision technologies[1-3], most of which use camera images, are widely used for recognizing 3-dimensional position and orientation of rigid bodies since they are effective and easily implemented. Many of computer vision approaches use landmarks designed to extract their features easily and accurately. These approaches can be effective means to locate mobile robots, to estimate their position and orientation, etc. However, they are hardly applied to precise measurements. The precision of computer vision approaches is limited to the order of a few millimeters or tenths of a millimeter.

We can see another 6-DOF sensor in master-slave mechanisms[4-6] that are widely used in tele-operation and virtual reality systems. In such systems, the kinematic parameters of master devices are identified and six encoders, either optical or magnetic types, measure the joint coordinates of each link. Through the forward kinematics of the master device, we can estimate the 3-dimensional position and orientation of the end-effector. Thus, master mechanisms are a kind of 6-DOF sensor. The order of precision of the master mechanisms is similar to that of computer vision sensors, a few millimeters or

Optomechatronic Systems, Hyungsuck Cho, George K. Knopf, Editors,
Proceedings of SPIE Vol. 4190 (2001) © 2001 SPIE · 0277-786X/01/$15.00

tenths of a millimeter.

Six degrees of freedom motion of aircraft, missiles, and rockets are estimated by inertial navigation systems(INS)[7-9]. INS measures linear and angular accelerations in 6-DOF and integrates them with respect to time to estimate the 3-dimensional position, x, y, and z-coordinates, and rotation, roll, pitch, and yaw-angles. These approaches needs no landmark as used in computer vision approaches and quite accurate for a while after initiation of integration. But errors in all of six components are accumulated and keep increasing as time goes. The accumulated errors are hardly bound to some limit values. Thus, these approaches are not proper to precise measurement either.

For precise measurement of position and rotation in the order of micrometers and micro-radians, optical instruments such as laser interferometer and laser doppler vibrometer are widely used[10-12]. These instruments show very high precision even in the order of nanometers in translation. These sensors are basically for one-dimensional measurement. For higher dimensional measurement such as two or three dimensional position plus rotation, it needs to integrate several laser interferometers and laser doppler vibrometers, which is a very difficult task and actually impossible for 6-DOF applications. Park et. al.[13] proposed to adopt a 3-facet mirror to measure 6-DOF displacement of objects in the precision order of a few micrometers in translation and a few micro radians in rotation. But it needs to mechanically control the laser beam position to trace the 3-facet mirror. Thus, it can not be applied to objects in high-speed motion.

In this paper, an advanced measuring system is proposed which can measure the 3-dimensional position and orientation of rigid bodies in the precision order of micrometers and micro-radians, and does not need mechanical control of laser beam position. This method has been motivated by Park et. al.'s previous method[13] that used a 3-facet mirror. For precise measurement, we utilize a laser source, a specially fabricated mirror, and three position-sensitive detectors(PSD). The specially fabricated mirror looks like a triangular pyramid having an equilateral cross-sectional shape, 3-facet mirror. Three PSDs are located at three corner points of a triangular formation, which is an equilateral triangular formation lying parallel to the reference plane. A laser beam is emitted from the He-Ne laser source located at the upright position and vertically incident on the top of the 3-facet mirror. The laser beam is reflected at the 3-facet mirror and splits into three sub-beams, each of which is reflected from the three facets and finally arrives at three PSDs, respectively. From the signals of the PSDs, we can calculate the 3-dimensional position and orientation of the 3-facet mirror, and can get the 3-dimensional position and orientation of any object simply by mounting the 3-facet mirror on the object. In this paper, we model the relationship between the 3-dimensional position and orientation of the object and the outputs of three PSDs. A series of experiments is performed to demonstrate the effectiveness and accuracy of the proposed method. The experimental results show that the proposed sensing system can be an effective means of obtaining 3-dimensional position and orientation of arbitrary objects.

2. PRINCIPLE OF SENSOR SYSTEM

2.1 System configuration

Figure 1 shows the overall configuration of the sensor system that we proposed for precise measurement of 3-dimensional position and orientation of objects. As shown in the figure, the sensor system is composed of a mirror of pyramidal shape, a He-Ne laser source, three position-sensitive detectors(PSD). In the figure, the laser beam is emitted from the He-Ne laser source located at the upright position and vertically incident on the top of a mirror of pyramid shape. The mirror is specially fabricated, which has an equilateral triangular cross-section as shown in Figure 2. We call this mirror 3-facet mirror since the mirror has three lateral reflective surfaces inclined 45° to its bottom surface. As shown in Figure 2, the laser beam is reflected at the 3-facet mirror and splits into three sub-beams.

As shown in the figure, three PSDs are located at three corner points of a triangular formation, which is an equilateral triangular formation lying parallel to the reference plane. The sensitive areas of three PSDs are oriented toward the center point of the triangular formation. The object whose position and orientation are to be measured is situated at the center with the 3-facet mirror on its top surface. Each reflective facet of the 3-facet mirror faces toward each PSD and the three laser beams reflected at the 3-facet mirror arrive at three PSDs, respectively. Since each PSD is a 2-dimensional sensor, we can acquire the information on the 6-DOF pose of the 3-facet mirror. If we mount the 3-facet mirror on any object, then we can also measure the 6-DOF pose of the object. The mathematical relationship between the 3-dimensional pose of the 3-facet mirror and the six outputs of the PSDs is to be explained in next section.

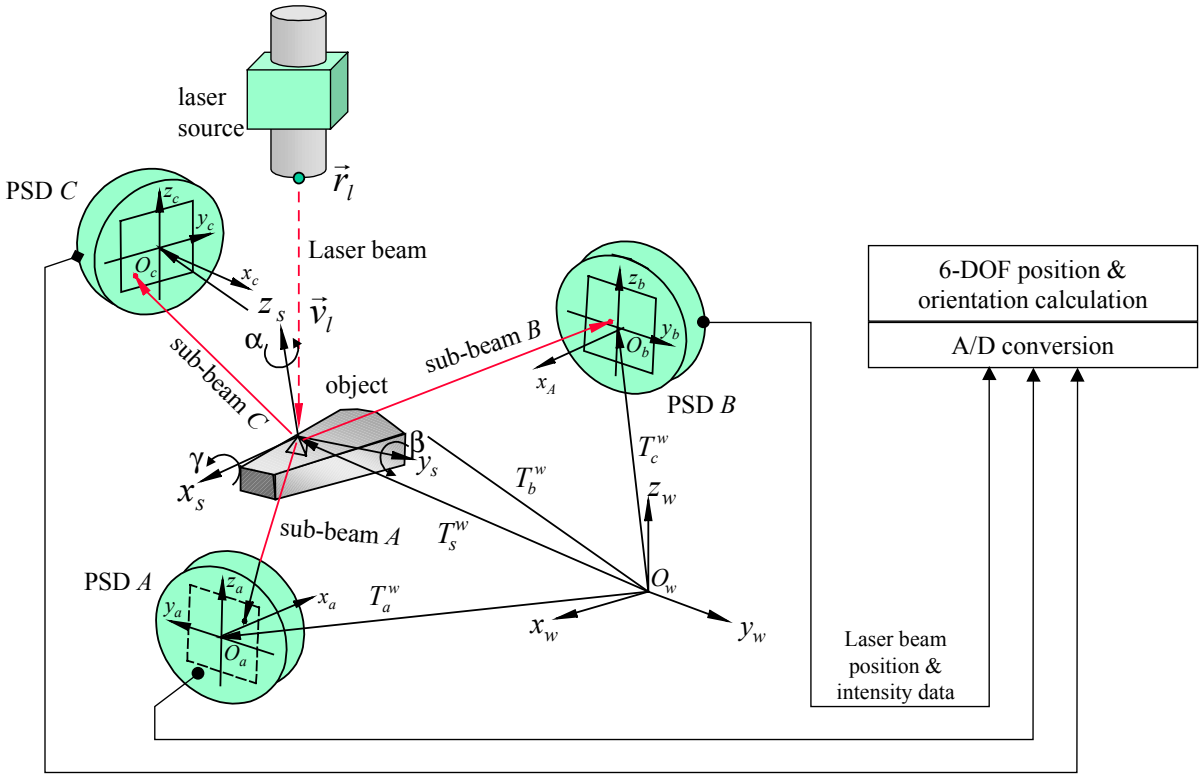

Figure 1 System configuration

As shown in Figure 1, each PSD gives us the 2-dimensional position of laser beam spot and its irradiant power. Thus, three PSDs give us totally nine outputs related with the positions of the laser beam spots and power data. Thus, for acquiring whole data, it needs an analog-to-digital(A/D) conversion board with at least nine channels. We can calculate the x, y, z translation and roll, pitch, yaw rotation from the six positional data and three irradiant power data through the sensor model to be presented in next section.

In the measurement system, the position and orientation of the laser beam are fixed to be constant and the laser beam should illuminates the top of 3-facet mirror. Thus, the position of 3-facet mirror needs to be restricted within the cross-section of laser beam so that the beam always covers the top of 3-facet mirror. We can see the laser beam from the laser source splits into three sub-beams so that each sub-beam shares the light power with each other.

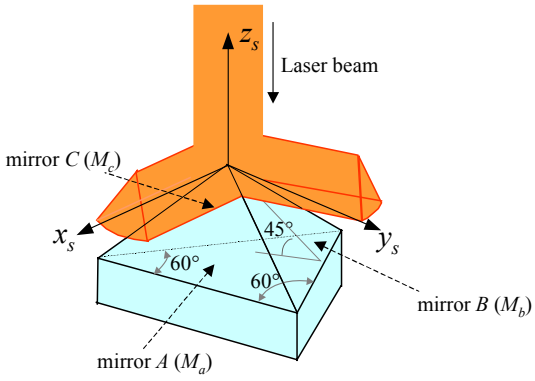

Figure 2 3-facet mirror reflecting a laser beam into three beams

2.2 Sensor model

To model the relationship between the 3-dimensional pose of the 3-facet mirror and the PSDs' outputs, we note the six positional and three power outputs of three PSDs with (ψ_a, ζ_a), (ψ_b, ζ_b), (ψ_c, ζ_c), Φ_a^*, Φ_b^*, and Φ_c^*, respectively. And we note 3-dimensional position and rotation of the 3-facet mirror with $\vec{t}^{\,w} = [t_x^w \quad t_y^w \quad t_z^w]^T$ and $\vec{\omega}^w = [\gamma \quad \beta \quad \alpha]^T$. In this paper, the sensor model calculates (ψ_a, ζ_a), (ψ_b, ζ_b), (ψ_c, ζ_c), Φ_a^*, Φ_b^*, and Φ_c^* from the given $\vec{t}^{\,w} = [t_x^w \quad t_y^w \quad t_z^w]^T$ and $\vec{\omega}^w = [\gamma \quad \beta \quad \alpha]^T$.

Figure 3 shows that a sub-beam reflected from M_a goes incident on *PSD A* to form an image looking like a piece of pie, say P_a. The 2-dimensional position (ψ_a, ζ_a) is the centroid of P_a weighted with intensity distribution of gaussian function. And laser power Φ_a^* is total power incident on *PSD A* that can be calculated through integration of intensity distribution over P_a. The calculation procedures for *PSD A* including *PSD B* and *C* are described as follows.

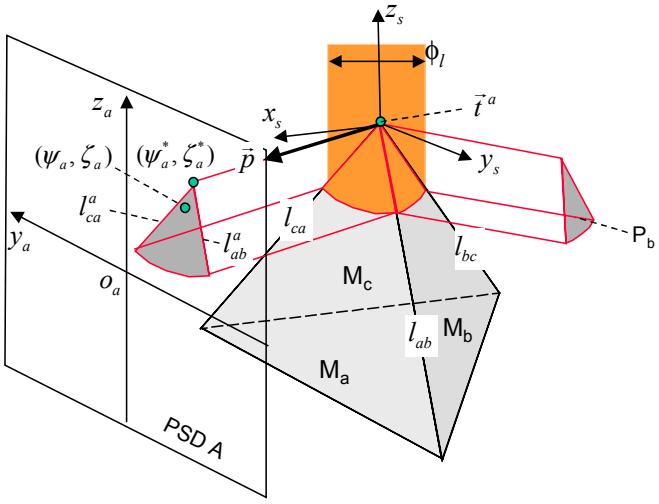

Figure 3 3-facet mirror reflecting a laser beam into *PSD A*

At first, we model the original laser beam on a gaussian beam from a source whose direction vector is $\vec{v}_l$ and the position of source point is $\vec{r}_l$. As described above, the direction of laser beam is kept to be vertical and the position is fixed. Thus, $\vec{v}_l$ and $\vec{r}_l$ can be expressed as Eqs. (1) and (2).

$$\vec{v}_l = [0 \quad 0 \quad -1]^T \tag{1}$$

$$\vec{r}_l = [0 \quad 0 \quad h]^T \tag{2}$$

Here, h represents the height of the laser source from system reference, which does not affect the system. And intensity within the laser beam assumed to be distrubuted as gaussian function as Eq. (3).

$$I(r) = \frac{8P}{\pi\phi_l^2} \exp\left(-\frac{8r^2}{\phi_l^2}\right) \tag{3}$$

Here, P represents the power of laser beam, ϕ_l the diameter of laser beam, and r the radial distance from the center axis of laser beam to any point of interest.

The vertex of P_a, (ψ_a^*, ζ_a^*), can be computed from intersection of the vertex of sub-beam A and *PSD A*. As for (ψ_b^*, ζ_b^*) and (ψ_c^*, ζ_c^*), similar procedures can be performed. It should be noted that any one of (ψ_a^*, ζ_a^*), (ψ_b^*, ζ_b^*) and (ψ_c^*, ζ_c^*) is not the projection of laser beam center. They are just the images of the vertex of 3-facet mirror. To obtain (ψ_a^*, ζ_a^*), the vertex of sub-beam A must previously calculated. The vertex of sub-beam A is a line from the vertex of 3-facet mirror and directed to (ψ_a^*, ζ_a^*). The direction vectors of the three sub-beams are calculated through the light reflection law after the geometrical models of three mirror surfaces are obtained. The mirror surfaces are modeled as 3-dimensional plane. As shown in Figure 2, the three mirror planes are modeled with respect to the reference frame, o_s, which is located at the top of the 3-facet mirror. The z-axis of o_s is vertical to the bottom surface of the 3-facet mirror and the x-axis is vertical to a bottom edge. We call the mirror, that faces in the direction of x-axis, mirror A, and the others mirror B and C, and denote M_a, M_b, and M_c.

The surface normal vectors of M_a, M_b, and M_c with respect to o_s are as follows.

$$\begin{aligned}
\vec{n}_a^s &= \begin{bmatrix} \frac{1}{\sqrt{2}} & 0 & \frac{1}{\sqrt{2}} \end{bmatrix}^T \\
\vec{n}_b^s &= \begin{bmatrix} -\frac{1}{2\sqrt{2}} & \frac{\sqrt{3}}{2\sqrt{2}} & \frac{1}{\sqrt{2}} \end{bmatrix}^T \\
\vec{n}_c^s &= \begin{bmatrix} -\frac{1}{2\sqrt{2}} & -\frac{\sqrt{3}}{2\sqrt{2}} & \frac{1}{\sqrt{2}} \end{bmatrix}^T
\end{aligned} \tag{4}$$

where $\vec{n}_a$, $\vec{n}_b$, and $\vec{n}_c$ are the surface normal vectors of M_a, M_b, and M_c, respectively, and the right superscript character "s" means that the vectors are represented with respect to the coordinate system defined at the top of 3-facet mirror, o_s. As 3-facet mirror rotates around any axis, the vectors rotate with respect to world coordinates system, o_w. Thus, the vectors should be expressed with respect to o_w as follows.

$$\begin{aligned}
l_a &= \frac{1}{\sqrt{2}}(c\alpha c\beta + c\alpha s\beta c\gamma + s\alpha s\gamma) \\
m_a &= \frac{1}{\sqrt{2}}(s\alpha c\beta + s\alpha s\beta c\gamma - c\alpha s\gamma) \\
n_a &= -\frac{1}{\sqrt{2}}(s\beta - c\beta c\gamma)
\end{aligned} \tag{5}$$

$$\begin{aligned}
l_b &= -\frac{1}{2\sqrt{2}}c\alpha c\beta + \frac{\sqrt{3}}{2\sqrt{2}}(c\alpha s\beta s\gamma - s\alpha c\gamma) + \frac{1}{\sqrt{2}}(c\alpha s\beta c\gamma + s\alpha s\gamma) \\
m_b &= -\frac{1}{2\sqrt{2}}s\alpha c\beta + \frac{\sqrt{3}}{2\sqrt{2}}(s\alpha s\beta s\gamma + c\alpha c\gamma) + \frac{1}{\sqrt{2}}(s\alpha s\beta c\gamma - c\alpha s\gamma) \\
n_b &= \frac{1}{2\sqrt{2}}s\beta + \frac{\sqrt{3}}{2\sqrt{2}}c\beta s\gamma + \frac{1}{\sqrt{2}}c\beta c\gamma
\end{aligned} \tag{6}$$

$$
\begin{aligned}
l_c &= -\frac{1}{2\sqrt{2}} c\alpha c\beta - \frac{\sqrt{3}}{2\sqrt{2}}(c\alpha s\beta s\gamma - s\alpha c\gamma) + \frac{1}{\sqrt{2}}(c\alpha s\beta c\gamma + s\alpha s\gamma) \\
m_c &= -\frac{1}{2\sqrt{2}} s\alpha c\beta - \frac{\sqrt{3}}{2\sqrt{2}}(s\alpha s\beta s\gamma + c\alpha c\gamma) + \frac{1}{\sqrt{2}}(s\alpha s\beta c\gamma - c\alpha s\gamma) \\
n_c &= \frac{1}{2\sqrt{2}} s\beta - \frac{\sqrt{3}}{2\sqrt{2}} c\beta s\gamma + \frac{1}{\sqrt{2}} c\beta c\gamma
\end{aligned} \tag{7}
$$

where $\vec{n}_a^w = [l_a \;\; m_a \;\; n_a]^T$, $\vec{n}_b^w = [l_b \;\; m_b \;\; n_b]^T$, and $\vec{n}_c^w = [l_c \;\; m_c \;\; n_c]^T$, and γ, β, and α are rolling, pitching, and yawing angles of 3-facet mirror, respectively, and where $c\alpha$, $s\alpha$, and $c\beta$ represent $\cos\alpha$, $\sin\alpha$, and $\cos\beta$, and so on.

From the above equations, we can get the direction vectors of the three sub-beams using light reflection law[14] as

$$
\begin{aligned}
\vec{v}_a^w &= [v_{ax} \;\; v_{ay} \;\; v_{az}]^T = M_a^w \vec{v}_l^w \\
\vec{v}_b^w &= [v_{bx} \;\; v_{by} \;\; v_{bz}]^T = M_b^w \vec{v}_l^w \\
\vec{v}_c^w &= [v_{cx} \;\; v_{cy} \;\; v_{cz}]^T = M_c^w \vec{v}_l^w
\end{aligned} \tag{8}
$$

where the reflection matrices of the three mirror surfaces are given by

$$
\begin{aligned}
\mathbf{M}_a^w &= \begin{bmatrix} 1-2l_a^2 & -2l_a m_a & -2l_a n_a \\ -2l_a m_a & 1-2m_a^2 & -2n_a m_a \\ -2l_a n_a & -2n_a m_a & 1-2n_a^2 \end{bmatrix} \\
\mathbf{M}_b^w &= \begin{bmatrix} 1-2l_b^2 & -2l_b m_b & -2l_b n_b \\ -2l_b m_b & 1-2m_b^2 & -2n_b m_b \\ -2l_b n_b & -2n_b m_b & 1-2n_b^2 \end{bmatrix} \\
\mathbf{M}_c^w &= \begin{bmatrix} 1-2l_c^2 & -2l_c m_c & -2l_c n_c \\ -2l_c m_c & 1-2m_c^2 & -2n_c m_c \\ -2l_c n_c & -2n_c m_c & 1-2n_c^2 \end{bmatrix}.
\end{aligned} \tag{9}
$$

$\vec{p}_x$, shown in Figure 3, is the direction vector of sub-beam *A* expressed with respect to the *PSD A*'s coordinate system, o_a. Therefore, $\vec{p}_x$ can be calculated by transforming $\vec{v}_a^w$ as follows;

$$
\vec{p} = [p_x \;\; p_y \;\; p_z]^T = R_a^{w-1} \vec{v}_a^w \tag{10}
$$

where R_a^w is the rotation transformation that can be defined by orientation of *PSD A*. The position of vertex of 3-facet mirror, $\vec{t}^{\,w}$, also can be expressed with respect to o_a through homogeneous transform[15] T_w^a.

$$
\vec{t}^{\,a} = [t_x^a \;\; t_y^a \;\; t_z^a \;\; 1]^T = T_w^a \vec{t}^{\,'w}. \tag{11}
$$

Here, T_w^a is the inverse transform of T_a^w shown in Figure 3 and $\vec{t}^{\,'w} = [t_x^w \; t_y^w \; t_z^w \; 1]^T$. From Eq. (12), we can compute the intersection between the vertex of sub-beam *A* and *PSD A* through analytic geometry,

$$
\psi_a^* = -\frac{p_y}{p_x} t_x^a + t_y^a, \qquad \zeta_a^* = -\frac{p_z}{p_x} t_x^a + t_z^a. \tag{12}
$$

Similarly, for *PSD B* and *C*,

$$\psi_b^* = -\frac{p_y}{p_x} t_x^b + t_y^b , \qquad \zeta_b^* = -\frac{p_z}{p_x} t_x^b + t_z^b \tag{13}$$

$$\psi_c^* = -\frac{p_y}{p_x} t_x^c + t_y^c , \qquad \zeta_c^* = -\frac{p_z}{p_x} t_x^c + t_z^c . \tag{14}$$

So far, we have the images of vertices of 3-facet mirror projected on three PSDs. In a similar way, we can compute the images of the laser beam center, which actually appear on only one PSD, but imaginary on the others. This is because actual beam center is reflected only one of three mirrors, M_a, M_b, and M_c. We denote the 2-dimensional coordinates of the images of beam center with (ψ_a^o, ζ_a^o), (ψ_b^o, ζ_b^o) and (ψ_c^o, ζ_c^o) for *PSD A*, *B*, and *C*, respectively.

As described above, the 2-dimensional position (ψ_a, ζ_a), (ψ_b, ζ_b), and (ψ_c, ζ_c) are the centroids of P_a, P_b, and P_c weighted with intensity distribution of gaussian function. Thus these can be computed by evaluating Eqs. (15), (16), and (17).

$$\psi_a = \frac{\iint_{P_a} y_a I_a(r_a) dy_a dz_a}{\iint_{P_a} I_a(r_a) dy_a dz_a}, \qquad \zeta_a = \frac{\iint_{P_a} z_a I_a(r_a) dy_a dz_a}{\iint_{P_a} I_a(r_a) dy_a dz_a} \tag{15}$$

$$\psi_b = \frac{\iint_{P_b} y_b I_b(r_b) dy_b dz_b}{\iint_{P_b} I_b(r_b) dy_b dz_b}, \qquad \zeta_b = \frac{\iint_{P_b} z_b I_b(r_b) dy_b dz_b}{\iint_{b} I_b(r_b) dy_b dz_b} \tag{16}$$

$$\psi_c = \frac{\iint_{P_c} y_c I_c(r_c) dy_c dz_c}{\iint_{P_c} I_c(r_c) dy_c dz_c}, \qquad \zeta_c = \frac{\iint_{P_c} z_c I_c(r_c) dy_c dz_c}{\iint_{P_c} I_c(r_c) dy_c dz_c} \tag{17}$$

where $I_a(r_a)$, $I_b(r_b)$, and $I_c(r_c)$ represent laser power distributions of gaussian beam on *PSD A*, *B*, and *C*, respectively, and are given by

$$I_a(r_a) = \frac{\vec{p} \cdot \hat{x}_a}{\|\vec{p}\|} I(r_a) \tag{18}$$

$$I_b(r_b) = \frac{\vec{q} \cdot \hat{x}_b}{\|\vec{q}\|} I(r_b) \tag{19}$$

$$I_c(r_c) = \frac{\vec{r} \cdot \hat{x}_c}{\|\vec{r}\|} I(r_c) \tag{20}$$

$$r_a = \sqrt{(y_a - \psi_a^o)^2 \frac{p_x^2}{p_x^2 + p_y^2} + (z_a - \zeta_a^o)^2 \frac{p_x^2}{p_x^2 + p_z^2}} \tag{21}$$

$$r_b = \sqrt{(y_b - \psi_b^o)^2 \frac{q_x^2}{q_x^2 + q_y^2} + (z_b - \zeta_b^o)^2 \frac{q_x^2}{q_x^2 + q_z^2}} \tag{22}$$

$$r_c = \sqrt{(y_c - \psi_c^o)^2 \frac{r_x^2}{r_x^2 + r_y^2} + (z_c - \zeta_c^o)^2 \frac{r_x^2}{r_x^2 + r_z^2}} \tag{23}$$

Here, $\vec{q} = [q_x \quad q_y \quad q_z]^T$ and $\vec{r} = [r_x \quad r_y \quad r_z]^T$ are the direction vectors of the vertices of sub-beam *B* and *C*.

The incident powers of three PSDs, Φ_a^*, Φ_b^*, and Φ_c^*, are the denominators of Eqs. (15), (16), and (17). However, laser beam power may vary due to its original instability. Thus, it is more reliable to use normalized laser power that can be easily calculated through Eqs. (24), (25), and (26).

$$\Phi_a = \frac{1}{P} \iint_{P_a} I_a(r_a) dy_a dz_a \tag{24}$$

$$\Phi_b = \frac{1}{P} \iint_{P_b} I_b(r_b) dy_b dz_b \tag{25}$$

$$\Phi_c = \frac{1}{P} \iint_{P_c} I_c(r_c) dy_c dz_c \tag{26}$$

Here, *P* is the total laser power that can be obtained by

$$P = \Phi_a^* + \Phi_b^* + \Phi_c^*. \tag{27}$$

So far, we have modeled the relationship between the 3-dimensional pose, i.e. t_x, t_y, t_z, γ, β, and α, and the three 3-tuples of PSD outputs, $(\psi_a, \zeta_a, \Phi_a)$, $(\psi_b, \zeta_b, \Phi_b)$, and $(\psi_c, \zeta_c, \Phi_c)$. Through Eqs. (15) ~ (17) and (24) ~ (26) we can calculate $(\psi_a, \zeta_a, \Phi_a)$, $(\psi_b, \zeta_b, \Phi_b)$, and $(\psi_c, \zeta_c, \Phi_c)$ with given t_x, t_y, t_z, γ, β, and α. When we perform actual measurement with the proposed sensor system, we have to perform the inversion of above sequences of calculation, i.e. calculation of t_x, t_y, t_z, γ, β, and α with given $(\psi_a, \zeta_a, \Phi_a)$, $(\psi_b, \zeta_b, \Phi_b)$, and $(\psi_c, \zeta_c, \Phi_c)$. This is performed through a numerical way, Newton's method[16], through which we have successfully got the solution, t_x, t_y, t_z, γ, β, and α, with given $(\psi_a, \zeta_a, \Phi_a)$, $(\psi_b, \zeta_b, \Phi_b)$, and $(\psi_c, \zeta_c, \Phi_c)$ in the experiments to be presented next section.

3. EXPERIMENTS

In order to verify the principle and effectiveness of the proposed measurement method, we have implemented an experimental system and performed a series of experiments. Figure 4 shows the experimental system. In the figure, the laser beam is artificially represented as straight lines, which is not shown by naked eyes in actual situation. Planar view of the experimental system is shown in Figure 5. In the figure, the 3-facet mirror is located at the origin of the reference frame, o_w. Three PSDs are equally far from the origin of o_w, one of which, *PSD A*, is located on the *x*-axis of o_w, and the others are located on the lines that make angles of 120° to the x_w axis. The frames, o_a, o_b, and o_c, are located at the centers of the PSDs, *PSD A*, *PSD B*, and *PSD C*, respectively, whose *x*-axes are directed toward the system origin, o_w.

The experiments include six sets of single axis movements and measurement, which include x_w, y_w, and z_w-translations, and rolling, pitching, and yawing. When x_w-axis movements are measured, the 3-facet mirror is sequentially positioned and

moved in x_w-direction while three PSDs' outputs, $(\psi_a, \zeta_a, \Phi_a)$, $(\psi_b, \zeta_b, \Phi_b)$, and $(\psi_c, \zeta_c, \Phi_c)$, are acquired. The movement is performed through actuating one of six axes of the 6-axis stage. For other axes such as y_w-translation, z_w-translation, rolling, pitching, and yawing, similar tasks are performed. The main parameters of the experimental system and the specifications of its components are listed in Table 1.

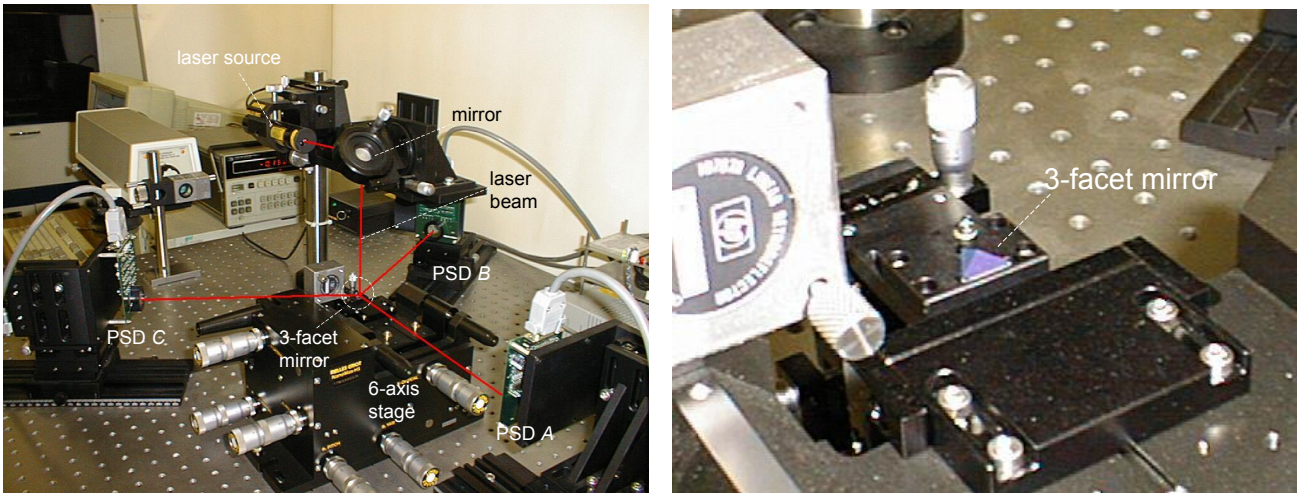

(a) (b)

Figure 4 Photograph of experimental system: (a) Whole system; (b) 3-facet mirror

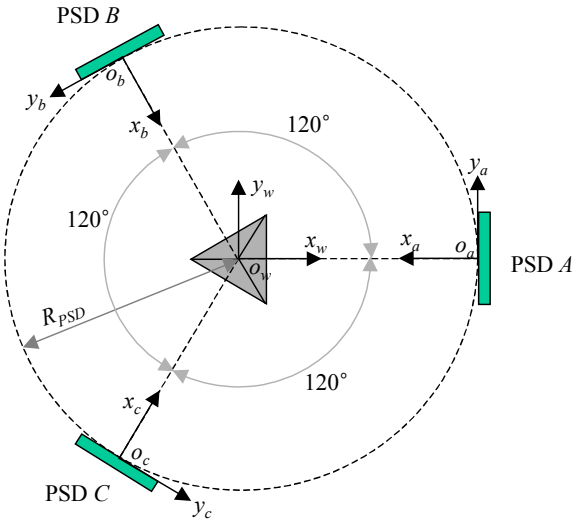

Figure 5 Layout and coordinate systems of the PSDs

Figure 6 and Figure 7 shows the experimental results for translations and rotations. Measured displacements, both positional and rotational, are plotted with respect to the reference values. On each point in the figures, data have been acquired twenty times, whose mean values are presented as well as the minimum and maximum values and the standard deviations. In Figure 6, we can see the measurement precision of the proposed sensor in case of linear translation. As shown in the figures, the ranges of the translations are very small. For x_w-translation, the position intervals of the data points are equally given as 13.5 μm, and for other directions such as y_w and z_w-translations, the intervals are 13.9 and 9.4 μm, respectively.

In Figure 7, the measurement results for *rolling, pitching,* and *yawing* movements are plotted. In rotation measurements such as rolling, pitching, and yawing, the angular intervals are given as 163 μrad, 158 μrad, and 158 μrad for

rolling, pitching, and *yawing*, respectively. As shown in Table 2, the relative uncertainties are smaller than those of translation measurements. The measurement precision of the proposed sensor for rotation is linearly proportional to the radial distance of PSDs from the system origin, o_w. If the distance gets two times then the precision of rotation measurement is improved by two times, but measurement range reduces by half.

Table 1 Specifications of the experimental system

Components	Specifications		
He-Ne Laser	Power		0.8 mW
	Beam diameter		0.97 mm
	Beam orientation at 3-facet mirror		Vertical (const.)
3-facet mirror	Azimuth of surface normal		45°
	Longitudinal distance between surface normals		120°
	Surface flatness		λ/10 at 632.8 nm
PSD	Size of sensitive area		13 mm x 13 mm
	Layout	Radial distance from the system origin	250 mm
		Longitudinal distance between PSDs	120°
		Orientations	See Figure 5

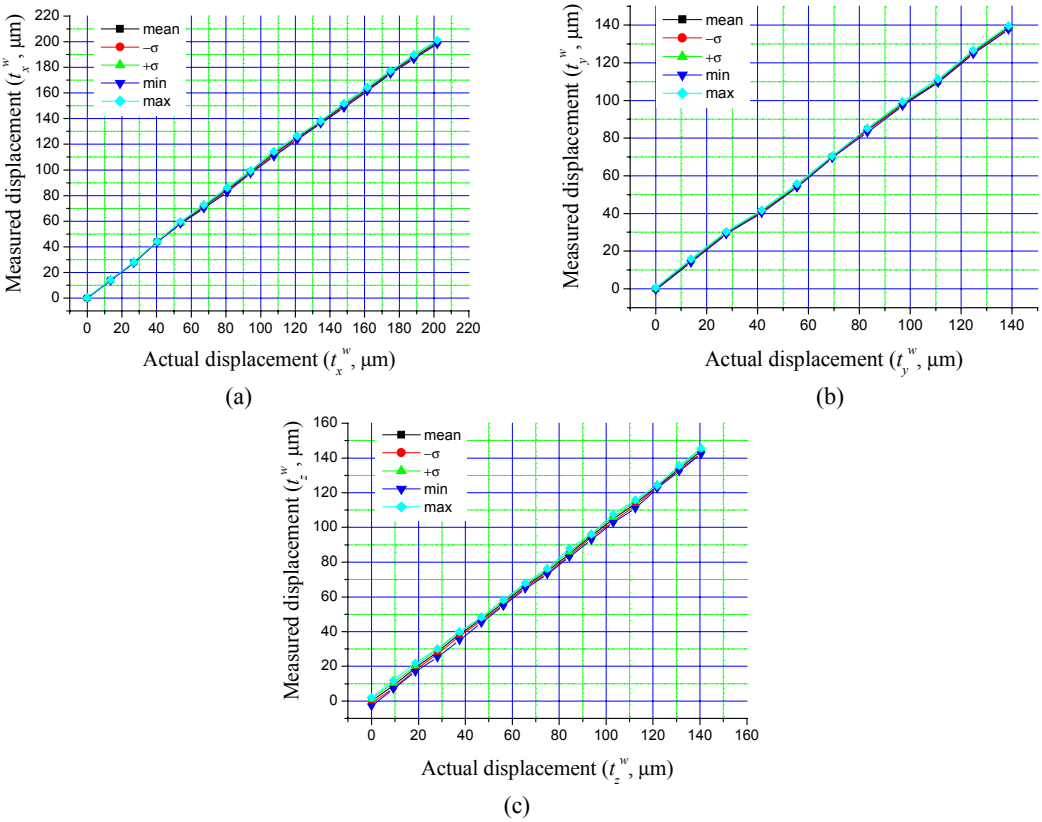

Figure 6 Measurement results of translation
(a) Measurement results of x_w-translation ; (b) Measurement results of y_w-translation; (c) Measurement results of z_w-translation

In Table 2, we can see the standard deviations, each of which is the median value out of the standard deviations calculated from every data point in each axis measurement. These represent the degree of precision for the relevant axis

movements in the sensor system. As shown in the table, the values are below 1.5μm for translations, and below 6.5 μrad for rotations. If there is a variation in the sensor reading of above two times of standard deviation in any axis, we can regard the 3-facet mirror as moving in the relevant direction with 95% probability. From this precision criterion, we can say the minimal movements in all 6-axis are 3μm for translations and 13μrad for rotations in the proposed sensor system.

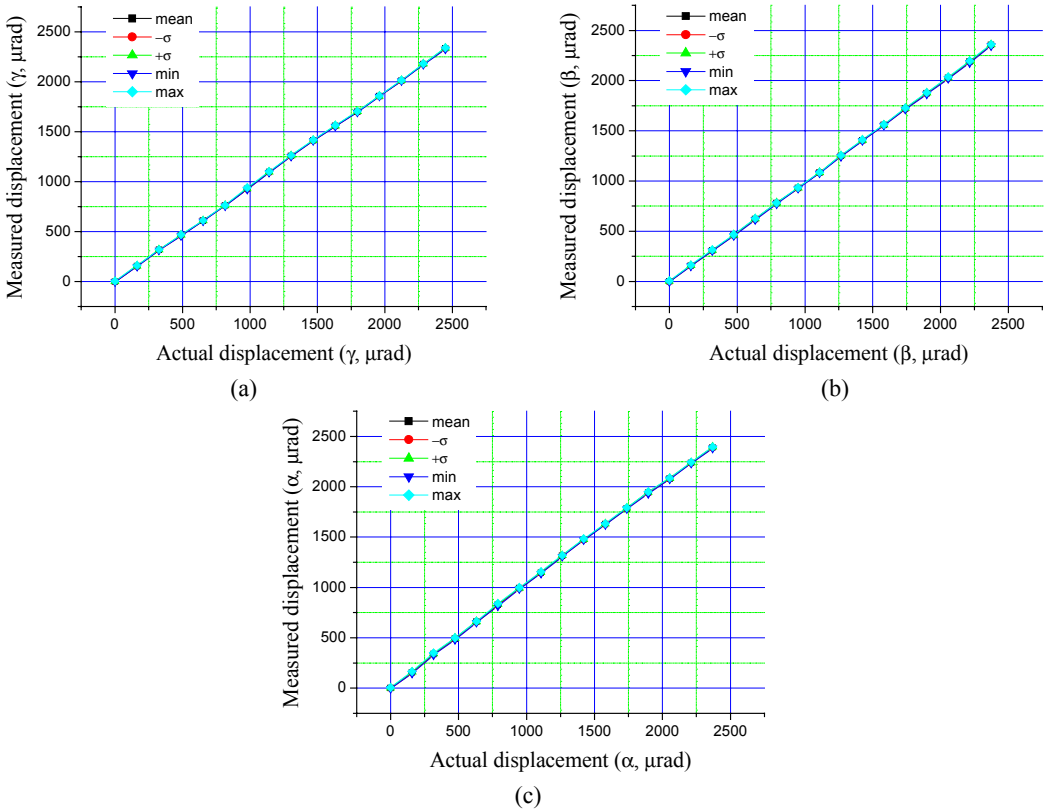

Figure 7 Measurement results of translation
(a) Measurement results of *rolling* ; (b) Measurement results of *pitching*; (c) Measurement results of *yawing*

Table 2 Measurement results (μm, μrad)

	Measured range	Measurement interval	Standard deviation	Relative uncertainty
x_w-translation (t_x)	202	13.5	1.31	3.4%
y_w-translation (t_y)	139	13.9	0.67	1.9%
z_w-translation (t_z)	141	9.4	1.41	3.6%
Rolling (γ)	2449	163	4.68	5.0%
Pitching (β)	2373	158	4.37	1.7%
Yawing (α)	2369	158	6.50	2.7%

4. CONCLUSION

In this paper, a new measurement system has been proposed to measure the 3-dimensional positions and orientations of rigid bodies in high precision. The proposed sensor system is based on laser optics which adopts a special mirror, 3-facet mirror, and a He-Ne laser, and three PSDs. The sensor system directly measures the 3-dimensional position and orientation of the 3-facet mirror mounted on objects in motion. In this paper, the laser light path in the system is mathematically modeled and the measurement principle is verified through a series of experiments.

The mathematical model is based on ray tracing, forward ray tracing in full, which traces the light path in the sensor system from the laser source to the destinations, three PSDs' surfaces, and yields three couples of 2-dimensional coordinates and powers of the laser beam spots on PSDs' surfaces. On the other hand, the inversion of the forward ray tracing is performed through a numerical method. The experiments have been performed for six fundamental motions such as x, y, z-translations, and roll, pitch, yaw-rotations. In the experiments, the 3-facet mirror is made to move at a small interval in each axis. Through the experiments, we could verify the measurement principle is valid and the proposed sensor system can measure the movements of any object in the precision of three micrometers in translation and thirteen micro-radians in rotation.

ACKNOWLEDGEMENT

This work has been performed as a part of the R&D project, Measurement of 6-DOF motion of HDD slider using a 3-facet mirror supported by Samsung Advanced Institute of Technology, Korea.

REFERENCES

1. A. Sulzmann and J. Jacot, “3D computer vision for microassembly stations and microfabrication,” *Proc. of the SPIE*, vol. 3202, pp. 42-51, 1998.
2. X. Du and S. C. Ahalt, “3D orientation vector estimation for subcomponents of space object imagery,” *Proc. of the SPIE*, vol. 3068, pp. 395-405, 1997.
3. S. H. Or, W. S. Luk, K. H. Wong, and I. King, “An efficient iterative pose estimation algorithm,” *Proc. of the Third Asian Conference on Computer Vision*, pp. 559-566, Hong Kong, 1998.
4. S. Tachi, T. Maeda, R. Hirata, and H. Hoshino, "A construction Method of Virtual Haptic Space," *Proc. of the Fourth Int. Conf. on Artificial Reality and Tele-Existence*, pp. 131-138, Tokyo, Japan, 1994.
5. H. Yokoi, J. Yamashita, Y. Fukui, and M. Shimojo, "Development of the virtual shape manipulating system," *Proc. of the Fourth Int. Conf. on Artificial Reality and Tele-Existence*, pp. 35-42, Tokyo, Japan, 1994.
6. A. Bejczy and K. Salisbury, "Kinematic coupling between operator and remote manipulator," *Advances in Computer Technology*, vol. 1, pp. 197-211, ASME, New York.
7. J. Vaganay, M. J. Aldon, and A. Fournier, “Mobile robot attitude estimation by fusion of inertial data,” *Proc. of IEEE Conference on Robotics and Automation*, pp. 277-282, 1993.
8. K. Komoriya and E. Oyama, “Position estimation of a mobile robot using optical fiber gyroscope,” *Proc. of Intelligent Robotic Systems*, pp. 143-149, 1994.
9. B. Barshan and H. F. Durrant-Whyte, “Evaluation of a solid-state gyroscope for robotics applications,” *IEEE Trans. Instrumentation and Measurement*, vol. 44, no. 1, 1994.
10. C. A. Briggs and F. E. Talke, “The dynamics of micro sliders using laser doppler vibrometry,” *IEEE Trans. Magnetics*, vol. 26, no. 5, 1990.
11. C. A. Briggs and F. E. Talke, “Investigation of the dynamics of 50% sliders using laser doppler vibrometry,” *IEEE Trans. Magnetics*, vol. 26, no. 6, 1990.
12. T. G. Jeong and D. B. Bogy, “Slider-disk interactions during the load-unload process,” *IEEE Trans. Magnetics*, vol. 26, no. 5, pp. 2490-2492, 1990.
13. W. S. Park, H. S. Cho, Y. K. Byun, N. Y. Park, and D. K. Jung, “Measurement of 3D position and orientation of rigid bodies using a 3-facet mirror,” *Proc. of SPIE Symp. on Intelligent Systems and Advanced Manufacturing*, vol. 3835, pp. 2-13, Boston, USA, 1999.
14. R. Kingslake, *Applied optics and optical engineering*, Academic Press., 1965.
15. John J. Craig, *Introduction to Robotics*, Addison Wesley, 1989.
16. Namir C. Shammas, *C/C++ Mathematical algorithms for scientists and engineers*, McGraw-Hill, 1996.